Chapter 10
"Digital Proxies" for Validating Models of Past Socio-ecological Systems in the Mediterranean Landscape Dynamics Project

C. Michael Barton, Isaac I. T. Ullah, Nicolas Gauthier, Nari Miller, Grant Snitker, Irene Esteban-Alamá, Joan Bernabeu Aubán, and Arjun Heimsath

10.1 Models in Archaeology

Recently, computational simulation modeling has been increasingly used in archaeology to represent and study the complex interactions among people and between people and environments (Kohler & van der Leeuw, 2007; Rogers & Cegielski, 2017; Romanowska et al 2021; Wurzer et al 2015). This approach offers sophisticated and transparent methods to study the invisible dynamics of past socio-ecological systems (SES) and test hypotheses about drivers of these dynamics, complementary to the analysis of the static behavioral residues that make up the archaeological record. We have often encountered criticism in reviews and informal comments from colleagues that such methods are "only models" and should be

C. M. Barton (✉)
School of Human Evolution and Social Change, School of Complex Adaptive Systems, Arizona State University, Tempe, AZ, USA
e-mail: Michael.Barton@asu.edu

I. I. T. Ullah
Department of Anthropology, San Diego State University, San Diego, CA, USA
e-mail: iullah@sdsu.edu

N. Gauthier
Laboratory of Tree-Ring Research and School of Geography, Development and Environment, University of Arizona, Tucson, AZ, USA

Scripps Institution of Oceanography, University of California San Diego, La Jolla, CA, USA

Florida Museum of Natural History, University of Florida, Gainesville, FL, USA
e-mail: ngauthier@arizona.edu

N. Miller · A. Heimsath
School of Earth and Space Exploration, Arizona State University, Tempe, AZ, USA

S. Pardo-Gordó, S. Bergin (eds.), *Simulating Transitions to Agriculture in Prehistory*, Computational Social Sciences, https://doi.org/10.1007/978-3-030-83643-6_10

taken as somehow less informative or meaningful than the empirical archaeological record. It must be noted, however, that the broken bits of trash that comprise this real-world record say nothing in and of themselves of ancient societal organization, practices, and environmental actions. Rather, interpretation of the archaeological record is used to reconstruct long-dead societies and their dynamics. These interpretive reconstructions are also "only models," whether in the form of natural language narratives, illustrations, maps, or graphs and whether the interpretations on which reconstructions of past SES are based on subjective intuition or quantitative analytics (Barton, 2013). That is, barring the invention of a time machine, a la H.G. Wells (1895) allowing for direct observation, we always have "only models" to represent the past systems that are the subject of archaeological inquiry.

Models are summary or abstract accounts of real-world phenomena and often also involve explanation. The most common models in archaeology are those that offer accounts of what happened, who did it, and where and when it took place. But especially in more recent archaeological scholarship, models also focus on how and why social and ecological phenomena happened as they did. Importantly, all archaeological models should be considered hypotheses. Even basic descriptive models of who, what, where, and when are not based on summarizing direct observations, but must be built on inference chains from the observable archaeological record to the invisible past that are often long, complicated, tenuous, and debated. Without the time machine of science fiction, we can never know the true past. But hopefully we can find ways to distinguish more likely, more realistic, and more useful models of the past from those that are less so (Barton, 2016; Box, 1979).

10.1.1 Validating Models

Validation involves evaluating the usefulness of a model, e.g., for representing particular processes or answering particular questions. An efficient way to differentiate more useful models from less useful ones is to use them to predict some aspect of the observable, empirical record (in this case the archaeological record) and then

G. Snitker
USDA Forest Service, Southern Research Station, Center for Forest Disturbance Science, Athens, GA, USA

Department of Anthropology, University of Georgia, Athens, GA, USA
e-mail: grant.snitker@uga.edu

I. Esteban-Alamá
ERAAUB, Departament d'Història i Arqueologia, Facultat de Geografia i Història, Universitat de Barcelona, Barcelona, Spain

Evolutionary Studies Institute, University of the Witwatersrand, Johannesburg, South Africa

J. Bernabeu Aubán
Grup d'investigació PREMEDOC, Departament de Prehistòria, Arqueologia i Història Antiga, Universitat de València, València, Spain
e-mail: jbauban@uv.es

assess the fit of the predicted results to the observed. Our inability to directly observe the past, together with the fragmentary and discontinuous nature of the archaeological record, means that we cannot realistically expect any model to predict in detail the fraction of the archaeological record we actually recover in most cases. A more productive strategy is to generate a number of reasonable alternative models and see which are better and worse matches (Chamberlin, 1890; Grimm et al., 2005). In that way, we can at least eliminate models that do a poor job of predicting the empirical record and narrow the universe of potentially useful models to those that do the best job – so we can refine them to do better.

While straightforward conceptually, this protocol is often difficult to apply in archaeological practice. Nearly all of our narrative reconstructions and even most of our quantitative models are about conditions and actions of ancient people. Certainly, the objects of the archaeological record were once part of a rich materiality in daily life. But nearly all of what ends up in the samples archaeologists collect no longer served this role. Archaeological empirical data consists mostly of trash that no longer played direct roles in people's lives when they were alive and has subsequently been altered or lost by diverse formation processes and time (Schiffer, 1987). While all archaeologists are aware of these facts, they are often paid less attention than deserved in practice. This makes validating models yet more difficult, even when they try to predict the material consequences of the structures and processes they treat.

It is tempting to think that the difficulty with validating models is largely related to the vagaries of subjective and interpretive narratives and can be minimized with more explicit mathematical or computational representations of models, but this is not the case. An example is the growing use of models from human behavioral ecology (HBE) in archaeology (Codding & Bird, 2015). Many of these robust, quantitative models were developed to explain and predict the behavior of non-human animals but have been translated with some success to account for the behavior of humans. These analytical devices have been evaluated against observable animal and human behavior and found to be widely useful in certain contexts like representing foraging or farming practices (Gremillion, 2002; Keene, 1983; Smith et al., 1983). But their outcomes are normally expressed in terms of the behavior of living humans and at time scales of months to minutes – not in units that resolve into the altered trash of the archaeological record nor time spans that match those of even the most detailed prehistoric records. This does not mean that they are not highly useful heuristics, but it makes them difficult to validate empirically for prehistoric societies using the archaeological record.

These validation issues are equally challenging for computational simulation models. These models can generate populations of computational agents or cellular landscapes representing past individuals, communities, their characteristics, and their locations. In effect, they generate the same kinds of scenarios found in narratives but rendered in more explicit, quantitative form. If we want to treat these models as complex hypotheses, we confront again the fundamental differences between the composition of the material archaeological record and the digital worlds created by computational models. One way to resolve this model/data dissonance has been to use the archaeological record to reconstruct past SES inferentially and compare those reconstructions to computationally generated representations of ancient SES (Barton et al., 2010; Kohler et al., 2012). Even when both models are sophisticated and explicit, this is unsatisfying from both logical and scientific perspectives. It is, in effect, testing a quantitative model by comparing it to an inferential, largely subjective model; there is no direct comparison of model to data.

We cannot change the nature of the archaeological record, of course, even with more sophisticated data recovery methods. It will always be largely composed of refuse, disconnected from direct involvement in the lives of the people who made and used it; preserved and found in a fragmentary, altered state; and dispersed and subsequently recovered discontinuously in time and space. But we can create models that can be more directly compared with this imperfect empirical record.

The best known mathematical and computational models in archaeology to have taken this latter approach are the ones simulating the dispersal of agropastoral systems across Europe in the mid-Holocene. This line of investigation was pioneered by Albert Ammerman and Luigi Cavalli-Sforza (1971). Their model generated data that predicted the location and timing of the first farmers across Europe. These results were then directly compared with the empirical record of the locations and dates of the earliest Neolithic sites in Europe. This work inspired numerous, increasingly sophisticated models taking a similar approach over subsequent decades, which have proven valuable for helping us understand multiple dimensions of the transition to food production in Europe (e.g., Fort et al. (2012) and Lemmen et al. (2011)). Beyond results that can directly be compared with the location and dates of sites, there have been few other attempts so far to create models that generate a "digital proxy record" that can be compared directly against the empirical one to evaluate complex computational models of past SES. Most of these have followed the spread of agricultural model approach of generating snapshot spatial distributions of a digital proxy record (Altaweel & Wu, 2010; Watts & Ossa, 2016). Yet, models can also generate information about system change through time, information that is essential to archaeological explanation (Barton et al., 2016; Freeman et al., 2017; Kohler et al., 2012; Perry & O'Sullivan, 2018; Riris, 2018). Here we describe a new approach to generating a digital proxy record of long-term change in SES that can be more directly compared with the empirical record.

10.2 The Mediterranean Landscape Dynamics Project

The Mediterranean Landscape Dynamics Project (MedLanD) is an international and interdisciplinary research project, begun in 2004 and supported by the US National Science Foundation, which aims to help us better understand long-term dynamic interactions between rural land use, landscapes, and the emergence of coupled SES (Barton et al., 2016). This work builds on prior collaborative research on long-term human land use in Mediterranean Spain (Barton et al., 1999; Bernabeu Aubán et al., 1999; García Puchol et al., 2008). The MedLanD Project integrates archaeological and paleoecological fieldwork with a multi-component computational modeling environment to simulate socio-ecological dynamics and feedbacks (the MedLanD Modeling Laboratory or MML). The empirical data collection program and MML have been described in detail in many other papers (Barton et al., 2010, 2012, 2015a, 2016; Barton, 2013; Mitasova et al., 2013; Robinson et al., 2018; Sarjoughian et al., 2015; Ullah, 2017; Ullah & Bergin, 2012), and we provide only a brief summary here.

10.2.1 MedLanD Modeling Laboratory

The MML dynamically couples different models as components in a meta-model environment: an agent-based model (ABM) of households practicing subsistence agriculture and/or pastoralism, cellular automata models of vegetation growth, soil fertility dynamics, and geomorphic landscape evolution (e.g., erosion/deposition) along with climate scenario data (Barton et al., 2010, 2015a, b, 2016; Mitasova et al., 2013). The components of the MML are connected through a coupler that both schedules events and passes information between components (Gholami et al., 2014; Mayer & Sarjoughian, 2009; Robinson et al., 2018; Sarjoughian et al., 2013, 2015) to permit high-resolution, realistic simulation of socio-ecological system dynamics.

The MML is designed as a configurable and controlled experimental environment to represent coupled human and natural systems (Miller & Page, 2007; van der Leeuw, 2004; Verburg et al., 2016). Villages and/or households comprise agents in the ABM to simulate land use decisions and behaviors of small-holder farming (Banning, 2010; Flannery, 1993; Kohler & van der Leeuw, 2007). These agents select land for cultivation and grazing using decision algorithms informed and parameterized by empirical studies of subsistence farming (Ullah, 2017). The MML is tuned to Mediterranean and xeric landscapes (Ullah, 2017) but could be parameterized to simulate small-holder agropastoralism in other environments. The landscape evolution model (LEM) iteratively evolves digital terrain, soil, and vegetation within a watershed by simulating sediment entrainment, transport, and deposition, and also tracks changes in soil depth and fertility due to cultivation and fallowing (Barton et al., 2016; Mitasova et al., 2013). A simple vegetation model simulates clearance for cultivation or removal by grazing and regrowth tuned to a Mediterranean 50-year succession interval based on empirical studies in the region (Bonet, 2004; Bonet & Pausas, 2007). Climate parameters, from modern or paleoclimate data or simulation, can be entered iteratively from a file or as a single set of values used for the entire simulation. Recently, we have added a component to model naturally occurring and anthropogenic landscape fire, to represent the use of fire by small-holder agropastoralists to clear land for cultivation or improve grazing for animals (Snitker, 2018).

10.3 Validating Socio-ecological Systems Models

10.3.1 Empirical Proxy Data and Analysis

Because the goal of the MedLanD Project is to understand long-term interactions between land use and landscapes, much of the associated archaeological fieldwork has focused on systematic, patch-based survey of numerous valleys in central eastern Spain to provide regional-scale empirical data related to long-term land use. This collaborative work has been jointly directed by researchers at the University of Valencia and Arizona State University and included both Spanish and American team members. This survey methodology is described in detail elsewhere (Barton et al., 1999; Bernabeu Aubán et al., 1999, 2006, 2014; Diez Castillo et al., 2008, 2014; García Puchol et al., 2014; Snitker et al., 2018). We have also carried out excavations and coring at occupational localities (Bernabeu Auban et al., 2003; Bernabeu Aubán & Orozco Köhler, 2005; Bernabeu, 1993; Bernabeu et al., 1994; García Puchol et al., 2008; García Puchol and Aura Tortosa, 2006) and extracted sediment columns at the outlets of watershed basins of varying size (Snitker, 2019). This work has produced a rich and extensive empirical archaeological record of long-term land use and socio-ecological dynamics (Barton et al., 1999, 2004b, c; Bernabeu Aubán et al., 1999, 2006, 2008; Diez Castillo et al., 2008).

In recent MedLanD fieldwork, we have collected columns of sediment samples from natural exposures in alluvial deposits at the outlets of selected watersheds. This innovative data collection protocol, developed by one of the co-authors (Snitker), is based on the recognition that such deposits represent a spatially averaged signal for a temporal sequence of landscape dynamics within the watershed basin upslope from the sampling location. By careful selection of locations at the outlets of differently located and different-sized watershed basins, these sediment columns can provide information about landscape processes – including erosion/deposition, vegetation, fires, and human land use – at multiple scales (Snitker, 2019). Sediment samples of approximately 1 liter in volume were collected in 5 cm levels within each column. The top 30 cm of each column was excluded as representing the modern plow zone. Sediment samples were subdivided for analysis. Micro-charcoal analysis was conducted on one subsample, phytoliths were extracted from another set, and a third set is currently being analyzed for long-term catchment-averaged erosion rates and sediment transport rates using cosmogenic nuclides (^{10}Be and ^{36}Cl).

For the preliminary model validation protocol described here, we selected one such sediment column (SP.NV.7) in the middle of the Canal de Navarrés valley (Fig. 10.1). Extending 2.35 m below the modern surface, SP.NV.7 produced 24 sediment samples below the modern plow zone (Table 10.1). Three radiocarbon dates were obtained for the column and were used to generate an age-depth model for all samples, using procedures described in Parnell et al. (2011, 2008) and the BChron package in R (Parnell et al., 2008). This model provided age estimates for all samples, for use in comparison with model output described below.

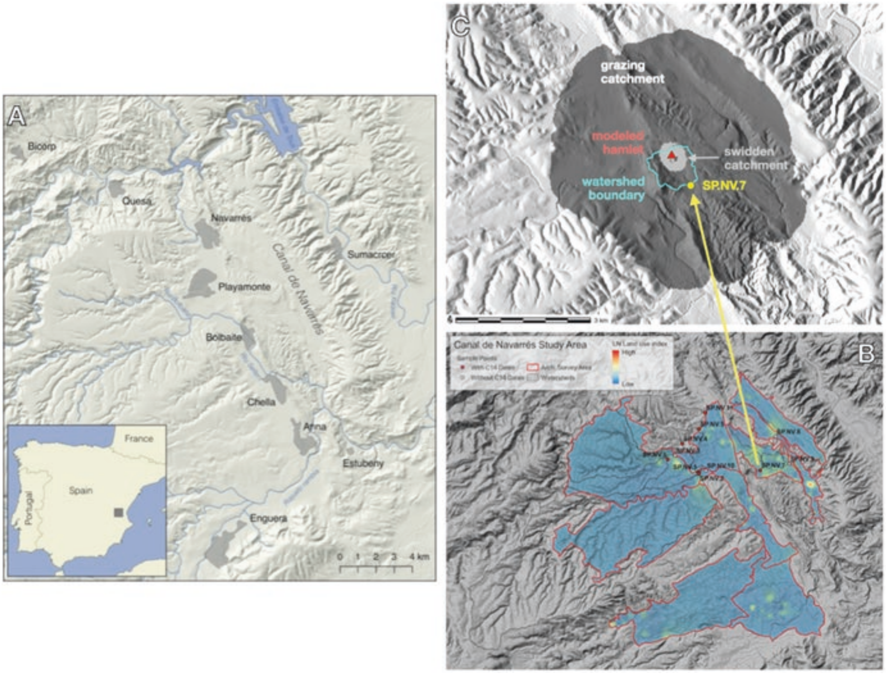

Fig. 10.1 (**a**) Location of Canal de Navarrés field work. (**b**) Archaeological survey zones and sediment column localities in Canal de Navarrés valley, overlay shading indicates estimated Neolithic land use intensity (see Snitker et al., 2018). (**c**) Parameterization for SES modeling, showing simulated hamlet, farming and grazing catchments, and boundary of watershed draining through location of core SP.NV.7

Phytoliths were extracted using standard methods described in Katz et al. (2010) and identified by Esteban (Table 10.2, Fig. 10.2). Descriptions and naming of the phytoliths follow the International Code for Phytolith Nomenclature 2.0 (Neumann et al., 2019). Diatoms and sponge spicules were also counted but not identified taxonomically. The sediments analyzed were deposited in periodically high-energy alluvial environments and contained a high proportion of sands and gravels, rather than in the low-energy environments normally preferred for micro-botanical studies. This posed several challenges for analysis and interpretation. To address this, prior to chemical extraction, sediment samples were sieved to a size fraction <0.025 cm due to the coarse character of the sandy sediments. Phytolith density was still very low, with most samples having <20,000 phytoliths per gram and a quarter of the samples lacking any phytoliths at all (Table 10.2). Additionally the coarse grain size and high-energy environment damaged many of the phytoliths that were recovered; weathered or otherwise unidentifiable phytoliths represented 10–70% (Table 10.2). As a result, the number of identifiable phytoliths was lower than what is normally desirable (Albert & Weiner, 2001); only two samples had more than 50 identifiable phytoliths after screening two slides. Because of the well-known relationship

Table 10.1 Chronology of core SP.NV.7. Radiocarbon dates and age-depth model calculated with BChron R package (Parnell et al., 2008, 2011)

Sample	Depth (cm BS)	Age-depth model (median age cal BP)	Period	^{14}C date (uncal BP)	^{14}C lab number
SP. NV.7.24	40–50	822	Medieval	692 ± 19	AA107775
SP. NV.7.23	90–100	2617	Iron Age		
SP. NV.7.22	100–110	2955	Bronze Age		
SP. NV.7.21	110–120	3299	Bronze Age		
SP. NV.7.20	120–130	3648	Bronze Age		
SP. NV.7.19	130–140	3990	Chalcolithic		
SP. NV.7.18	140–150	4341	Chalcolithic		
SP. NV.7.17	150–155	4599	Late Neolithic		
SP. NV.7.16	155–160	4776	Late Neolithic		
SP. NV.7.15	160–165	4958	Late Neolithic		
SP. NV.7.14	165–170	5167	Late Neolithic		
SP. NV.7.13	170–175	5400	Late Neolithic	4586 ± 71	AA109784
SP. NV.7.12	175–180	5632	Late Neolithic		
SP. NV.7.11	180–185	5871	Late Neolithic		
SP. NV.7.10	185–190	6112	Middle Neolithic		
SP. NV.7.09	190–195	6343	Middle Neolithic		
SP. NV.7.08	195–200	6572	Middle Neolithic		
SP. NV.7.07	200–205	6803	Early Neolithic		
SP. NV.7.06	205–210	7036	Early Neolithic		
SP. NV.7.05	210–215	7273	Early Neolithic		
SP. NV.7.04	215–220	7509	Early Neolithic		
SP. NV.7.03	220–225	7744	Late Mesolithic		

(continued)

Table 10.1 (continued)

Sample	Depth (cm BS)	Age-depth model (median age cal BP)	Period	^{14}C date (uncal BP)	^{14}C lab number
SP. NV.7.02	225–230	7986	Late Mesolithic		
SP. NV.7.01	230–235	8237	Late Mesolithic	7559 ± 46	AA110530

between diversity and sample size, taxonomic diversity is probably underrepresented, especially for rare morphotypes (Zurro, 2018). For this reason, we grouped phytolith morphotypes into broad ecological categories, rather than more specific taxa: grasses (grass silica short cells and elongates with decorated margins), herbaceous plants (elongates and acute bulbous phytoliths), woody plants including trees and shrubs (blocky, bocky polyhedral, spheroids psilate, sclereid, tracheary, and platelets), and riparian plants (papillate and spheroid echinate) (Table 10.2, Fig. 10.2). These ecological groups were sufficient for comparisons with modeling output (see below), allowing us to calculate a simple index of land cover change as woody plant phytoliths/open vegetation phytoliths (grasses + herbaceous) (Fig. 10.3). This should not be taken as a direct, quantitative indicator of the relative proportion of trees and shrubs to grasses and herbaceous plants. The absolute number of phytoliths is affected by the biogenic processes that create phytoliths from dead plant matter and subsequent depositional circumstances (i.e., alluvial transport mentioned above) that embedded them in the sampled sediments. Rather, this index should be seen as a more general estimate of the changing relative importance of woody to open vegetation in the watershed that drains through SP.NV.7. That said, the overwhelming dominance of woody plants in the phytolith record suggests that trees and shrubs were a significant, though fluctuating, component of the land cover in the watershed.

Charcoal was extracted using methods described in Snitker (2019) and analyzed by Snitker, using semi-automated digital identification and counting software he developed (Snitker, 2020). Following methods used in Snitker’s doctoral research, charcoal fragments were classified into four morphotypes, two of which represented woody and grass/herbaceous plants (Table 10.3, Fig. 10.2). Because of the above-mentioned depositional environments, the number of charcoal fragments recovered from each sample also was low, as is the case for phytoliths. Especially relevant is the apparent destruction of the more fragile morphotypes in the high-energy alluvial environments, especially elongated forms associated with grasses and other open vegetation communities. The consequence of the very low number of these morphotypes (Table 10.3) and overall low sample sizes is that we cannot meaningfully calculate even a land cover index like the one calculated for phytoliths. Nonetheless, the overwhelming dominance of charcoal from woody plants throughout the sequence is not in conflict with the phytolith record, in which woody plants are well represented. However, we were able to compare changes in the overall density of charcoal accumulation with modeled charcoal accumulation.

Table 10.2 Phytolith morphotypes identified and total phytolith concentrations from core SP.NV.7

	Grasses		Herbaceous		Woody			Riparian					
Sample	Grass	Long cells	Elongates	Epidermal appendages	Dicots	Blocky	Spheroids	Sedges	Decorated Spheroids	Unidentified	Weathered	Total phytoliths counted	Phytolith concentration per gm sediment
SP. NV.7.23	2	1	0	1	1	0	2	1	4	1	3	**16**	**11,091**
SP. NV.7.22	1	0	1	1	0	0	0	0	1	4	0	**8**	**12,055**
SP. NV.7.21	0	0	0	0	0	0	0	0	0	0	0	**0**	**0**
SP. NV.7.20	5	0	1	1	0	0	0	0	3	1	0	**11**	**22,634**
SP. NV.7.19	0	0	0	0	0	0	0	0	0	0	0	**0**	**0**
SP. NV.7.18	2	1	0	2	0	1	10	0	3	10	6	**35**	**16,976**
SP. NV.7.17	5	0	1	0	0	0	3	0	1	2	3	**15**	**18,083**
SP. NV.7.16	6	2	8	5	2	1	24	0	6	7	3	**64**	**10,664**
SP. NV.7.15	6	0	5	3	0	3	12	0	1	13	10	**53**	**5899**
SP. NV.7.14	6	1	5	1	0	2	18	0	6	13	9	**61**	**21,747**
SP. NV.7.13	0	0	0	0	0	0	0	0	0	0	0	**0**	**0**
SP. NV.7.12	3	0	2	0	1	0	4	0	11	14	15	**50**	**10,873**

	Grasses		Herbaceous		Woody			Riparian					
Sample	Grass	Long cells	Elongates	Epidermal appendages	Dicots	Blocky	Spheroids	Sedges	Decorated Spheroids	Unidentified	Weathered	Total phytoliths counted	Phytolith concentration per gm sediment
SP. NV.7.11	0	0	1	0	0	0	0	0	0	0	1	**2**	**6**
SP. NV.7.10	1	0	1	0	0	0	3	0	1	0	2	**8**	**5659**
SP. NV.7.09	0	0	0	0	0	0	0	0	0	0	0	**0**	**0**
SP. NV.7.08	5	0	2	0	0	0	7	0	2	2	5	**23**	**5776**
SP. NV.7.07	5	1	4	8	1	4	8	0	10	9	20	**70**	**16,636**
SP. NV.7.06	0	0	0	0	0	0	0	0	0	0	0	**0**	**0**
SP. NV.7.05	9	3	5	3	1	6	10	1	14	15	11	**78**	**32,620**
SP. NV.7.04	0	0	0	0	0	0	0	0	0	0	0	**0**	**0**
SP. NV.7.03	2	0	0	1	0	0	6	0	1	2	1	**13**	**5659**
SP. NV.7.02	0	0	0	0	0	0	0	0	0	0	0	**0**	**0**
SP. NV.7.01	0	0	0	0	0	0	0	0	0	0	0	**0**	**0**

Fig. 10.2 Empirical proxy data from core SP.NV.7, Canal de Navarrés valley, Valencia, Spain: phytolith and charcoal morphotypes (see also Tables 10.2 and 10.3)

10.3.2 Modeling Experiments and Digital Proxies

Output from the MML is primarily in the form of cellular raster grids representing "digital landscapes," including the vegetation cover, land use, soil depth, overland hydrological flow, net erosion-deposition, locations of fire (both lightning and human caused), and surface topography at each time step of the simulation, plus text files likewise documenting demographic, subsistence, and economic dynamics of agent households and villages over the course of the simulation (Fig. 10.4). However, the diverse empirical dataset recovered in MedLanD Project fieldwork – including bags of sediment, extracted fragments of charcoal, plant silica phytoliths, collections of stone artifacts, and fragments of ceramic vessels – bears no resemblance to these digital representations of land use, landscapes, and inhabitants simulated by the MML. Because we cannot change the nature of the empirical archaeological record, we have modified the MML to produce output that more closely matches the empirical data.

For the preliminary test of this validation protocol, we identified a raster cell equivalent to the location of the SP.NV.7 sediment core on a high-resolution DEM of the Canal de Navarrés valley (based on 5 m LiDAR data from the Valencian government). We then mapped the watershed basin that drained through this locale using hydrological modeling tools in GRASS GIS (Fig. 10.1). Our survey and analytical methods enable us to estimate changing spatial patterns of occupational intensity through time (Barton et al., 1999, 2004a; Snitker et al., 2018). We identified a region of higher occupational intensity for the early Neolithic within the boundaries of the watershed that drained through core sampling location and used a raster cell within this region as the location of a modeled farming hamlet to parameterize the MML (Fig. 10.1).

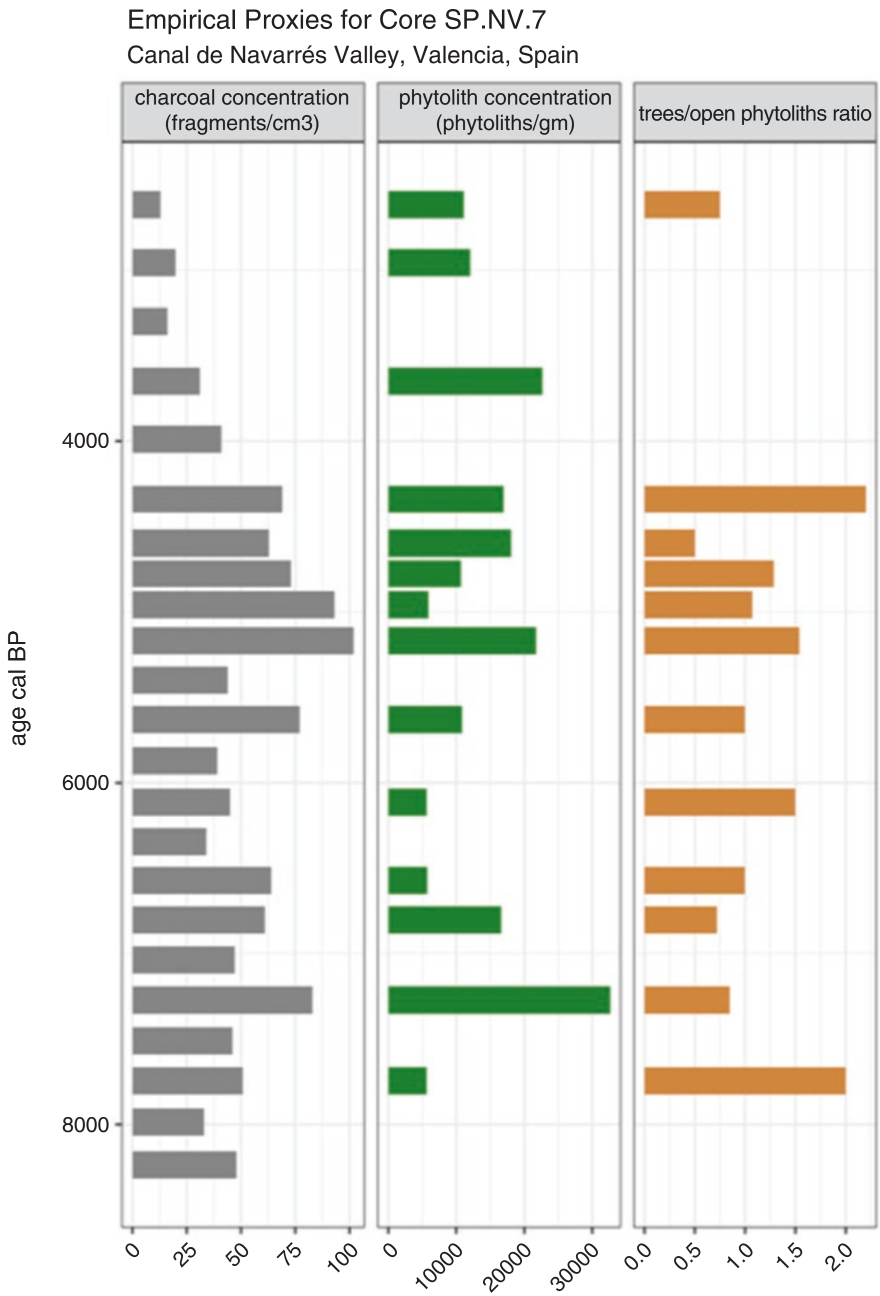

Fig. 10.3 Empirical proxy data from core SP.NV.7, Canal de Navarrés valley, Valencia, Spain: concentrations and ratio of woody to open vegetation phytoliths

Table 10.3 Charcoal morphotypes identified and total charcoal fragments from core SP.NV.7 (fragments per cm^3)

Sample	Geometric (woody plants)	Elongated (grass)	Irregular	Indeterminate	Total
SP.NV.7.24	0	0	0	0	0
SP.NV.7.23	8	0	2	3	**13**
SP.NV.7.22	9	0	3	8	**20**
SP.NV.7.21	10	0	5	1	**16**
SP.NV.7.20	5	0	11	14	**31**
SP.NV.7.19	16	1	16	8	**41**
SP.NV.7.18	16	0	33	20	**69**
SP.NV.7.17	5	1	44	13	**63**
SP.NV.7.16	33	1	28	11	**73**
SP.NV.7.15	53	0	33	7	**93**
SP.NV.7.14	35	0	48	19	**102**
SP.NV.7.13	10	0	22	12	**44**
SP.NV.7.12	24	0	42	11	**77**
SP.NV.7.11	4	1	26	8	**39**
SP.NV.7.10	17	0	24	4	**45**
SP.NV.7.09	8	1	15	10	**34**
SP.NV.7.08	17	0	30	17	**64**
SP.NV.7.07	13	0	28	20	**61**
SP.NV.7.06	10	0	23	14	**47**
SP.NV.7.05	20	0	47	16	**83**
SP.NV.7.04	7	0	29	10	**46**
SP.NV.7.03	12	0	36	3	**51**
SP.NV.7.02	11	0	19	3	**33**
SP.NV.7.01	17	0	25	6	**48**

When initialized with a raster digital elevation model (DEM) that matches a real-world landscape, the MML will simulate human and natural processes and consequent changes to that landscape over time. Beginning with the modeled farming hamlet on a DEM that corresponds to the Canal de Navarrés valley, we set up a series of four modeling experiments with two different agropastoral subsistence strategies and two control runs without human land use (Table 10.4).

For both experiments with human land use, we parameterized a farming hamlet with 120 individuals who satisfy their caloric needs through a combination of farming and ovicaprine herding. Following parameterizations detailed in Barton et al. (2015a), we calculated farming and grazing catchments for a crop-oriented subsistence strategy, where 80% of needed calories come from cereal agriculture and 20% from ovicaprines, and for a pastoral subsistence strategy, where 20% of needed calories come from cereal agriculture and 80% from ovicaprines. Farming catchments were subsequently calculated assuming shifting cultivation and a preference for land within walking distance with a slope of ≤10° (Barton et al., 2015a; Bevan & Conolly, 2004); grazing catchments were more extensive but within an 8-hour

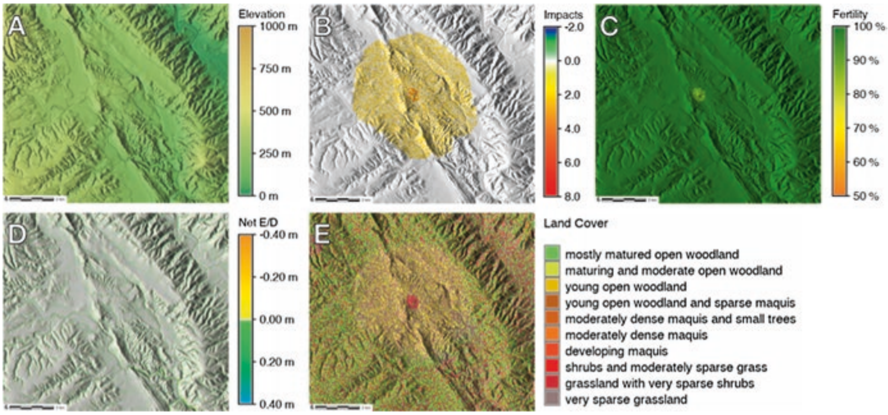

Fig. 10.4 Example raster output from the MedLanD Modeling Laboratory SES model (see text). Year 10 of agricultural scenario experiment (Table 10.4, Scenario 3). (**a**) High-resolution (5 × 5 m) LiDAR DEM of topography. (**b**) Human land use impacts (scale indicates decrease or increase in land cover value due to swidden farming or ovicaprine grazing). (**c**) Soil fertility (scale in percent of original fertility prior to human land use). (**d**) Net erosion or deposition for year 10 in each cell (scale in meters of accumulation or loss). (**e**) Land cover vegetation (scale in range of 0–50)

walking distance and without regard for slope (see Fig. 10.1). Fallow intervals and grazing intensity respond dynamically to changing community caloric needs, farming and grazing returns, and available labor during a simulation run (see Robinson et al., 2018). The simulation assumes that people used fire to clear land for cultivation; each time a cell is cleared, it generates digital micro-charcoal based on the vegetation growing on the cell at that time step. Additionally, lightning-caused fires are generated stochastically, based on topography and probability of storms (empirically determined from regional weather data) (IVIA, 2015; see Snitker, 2018).

In most MML modeling work, we run control experiments without humans in order to better evaluate the net impacts of human land use (Barton et al., 2010, 2015a, 2016). Here, we ran two control experiments: one with initial vegetation cover equivalent to Mediterranean woodland and another with initial vegetation equivalent to Mediterranean *matorral* shrubland. Lightning-caused fires were simulated as above, but we did not simulate anthropogenic fire in these two control experiments. In all four modeling experiments, rainfall was parameterized to mid-Holocene estimates, based on paleoclimate modeling.

Because the MML produces the abovementioned suite of raster landscape data for each yearly time step, it is possible to calculate for any given location (i.e., any specific raster cell in the digital landscape) a time series of the accumulation of sediment, depositional hiatuses, and erosional unconformities with an annual temporal resolution across an entire model run. We developed software that analyzes all of these rasters and employs transfer functions (Le & Shackleton, 1994) at each time step to mathematically transform values for simulated land use into "digital artifact" concentrations and transform simulated vegetation cover into "digital plant

Table 10.4 Modeling experiments conducted. Each experiment was repeated 40 times. One repetition from each experiment was selected as an example for discussion in this paper

	Scenario 1	Scenario 2	Scenario 3	Scenario 4
Initial vegetation	Mediterranean woodland	Sparse *matorral*	Mediterranean woodland	Mediterranean woodland
Human impact	None	None	80% swidden, 20% ovicaprine herding	20% swidden, 80% ovicaprine herding
Fires	Lightning only	Lightning only	Anthropogenic and lightning	Anthropogenic and lightning

phytoliths"; if fire is present, they also transform simulated vegetation cover into micro-charcoal.

For artifacts, all raster cells with simulated ovicaprine grazing generate 0–2 (randomly selected) units of artifacts each year. All raster cells with simulated farming generate double the artifact units generated by grazing each year (0–4). Because we do not have empirical artifact data in the form of micro-artifacts from the SP.NV.7 sediment column, we have not scaled or compared these values with empirical ones here.

Digital phytoliths are generated based on the proportions of open and woody vegetation, based on the land cover simulated by the MML. All but one of the four modeling experiments began with a land cover of Mediterranean woodland, including trees with an understory of shrubs and grasses/herbs. The fourth began with a land cover of *matorral* shrubland, also with a grass/herb understory. For each time step, the proportion of open vegetation (ranging from 40% to 100% coverage of a cell) is multiplied by 2 g/m^2, an empirically calculated rate of grass phytolith production in grassland (Fredlund & Tieszen, 1994). Because this rate is based on steppe rather than Mediterranean environments, it may be somewhat high for the Canal de Navarrés. But in spite of studies of phytolith production in Mediterranean landscapes (e.g., Tsartsidou et al., 2007), we have been unable to find other data on phytolith generation rates that can be used to parameterize our modeling. The proportion of woody vegetation (ranging from 0% to 100% coverage) is multiplied by 0.02 g/m^2 to represent the approximately two orders of magnitude lower phytolith production by woody plants (Albert & Weiner, 2001; Esteban et al., 2017; Tsartsidou et al., 2007; Esteban unpublished data from L'Estret de les Aigües, Xàtiva, Spain). The production rate of open and woody vegetation digital phytoliths is then multiplied by the area of each cell to create a map of grams per cell for each of these two digital phytolith types for each yearly time step.

The digital charcoal model uses maps of vegetation cover and lightning-caused fires, as well as maps of simulated farming and grazing for modeling experiments with anthropogenic land use. Vegetation cover is rescaled to aboveground plant biomass (0–1.95 kg/m^2) (Barton et al., 2015a; Ullah, 2017). This is multiplied by the proportion of plant biomass that produces charcoal fragments when burned (from 0.0048 for grasses and herbaceous plants to 0.0325 for trees) and divided in half to represent the amount of charcoal large enough to be identified (Carter et al., 1998; Flinn et al., 1979; Forbes et al., 2006). This is the amount of digital charcoal generated by any cell that is farmed or has a natural fire. Cells that are grazed only generate charcoal at 0.05 times the rate described above. The results are then rescaled into g/cell-like phytoliths.

Finally, the digital artifacts and ecofacts are accumulated in deposition or lost to erosion simulated for each cell and converted to a standard volumetric concentration in g/cm^3 of sediment for each cell. To make digital phytolith concentrations more directly comparable with empirical measures, we rescale further to phytoliths per grams of sediment using a bulk soil density of 1.2184 g/cm^3 and mean phytolith weight of 0.000011161 g estimated from Zurro (2018). For comparison with empirical micro-charcoal, we rescale the digital proxy output to fragments/cm^3, using a mean fragment weight of 0.00011304 g (Clark, 1988). This rescaling provides the data to more directly compare the results of complex SES modeling with empirical data recovered in fieldwork. Below, we describe a preliminary test of the analytical workflow for this novel model validation instrument.

10.4 Results and Validation Tests

We report here on an initial test of proxy modeling protocols and the potential for a digital core to be compared with an empirical core or sediment column to help validate complex SES model results. We ran each modeling experiment for 500 annual time steps and repeated each experiment 40 times. For the comparison reported here, we selected 1 of the 40 repetitions from each of the four experiments and generated an exemplar digital core to compare with SP.NV.7. The age-depth model allows us to identify a section of the empirical sediment column SP.NV.7 that spans the initial Neolithic occupation of the Canal de Navarrés valley to be roughly contemporaneous with the period represented by the simulation (though see below).

To create a more direct comparison with this section of the empirical sediment column, we bin the stratigraphically accumulated digital phytoliths and charcoal described above into 10 cm levels, aggregating the proxy accumulation within each level. We also calculate and aggregate the watershed basin average of the proxies for each level and add it to the level total for the outlet cell (i.e., digital core location) to simulate the combined in situ and exogenous contributions of digital proxies to each 10 cm level (see Fredlund & Tieszen, 1994). For comparison with empirical phytoliths, we calculated a simple index of land cover change as the ratio of woody vegetation/open vegetation per level for "digital phytoliths" (Figs. 10.8, 10.9, and 10.10).

Some of these 10 cm digital units span simulated erosional gaps in the digital sediment record in an analogous way to sampling of real-world sediment columns. We assigned ages to each digital 10 cm sampling unit based on the model annual time step that corresponded to the sediment accumulation at the midpoint of each, analogous to age-depth models for real-world sediment columns. Finally, a calendar age was assigned to each level, based on the assumption that each model run began at 7500 cal BP and each model time step is equivalent to a calendar year (but see below). The results are shown in Figs. 10.5, 10.6, 10.7, 10.8, 10.9, and 10.10. Note

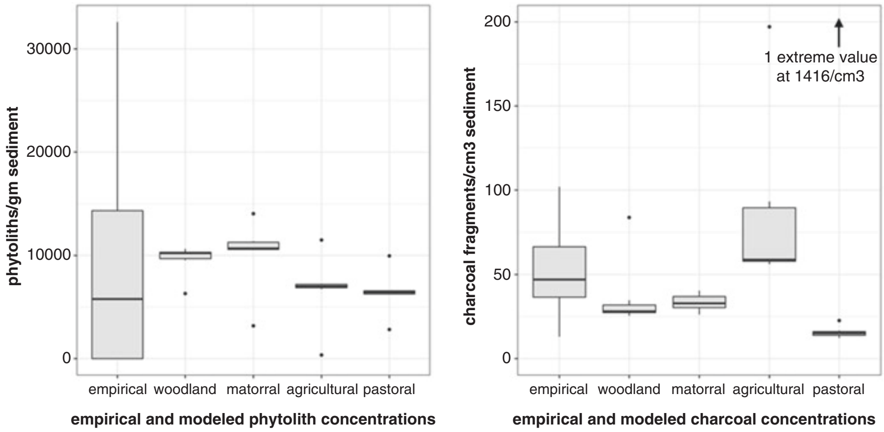

Fig. 10.5 Comparisons of concentrations of empirical proxies from core SP.NV.7 and modeled digital proxies

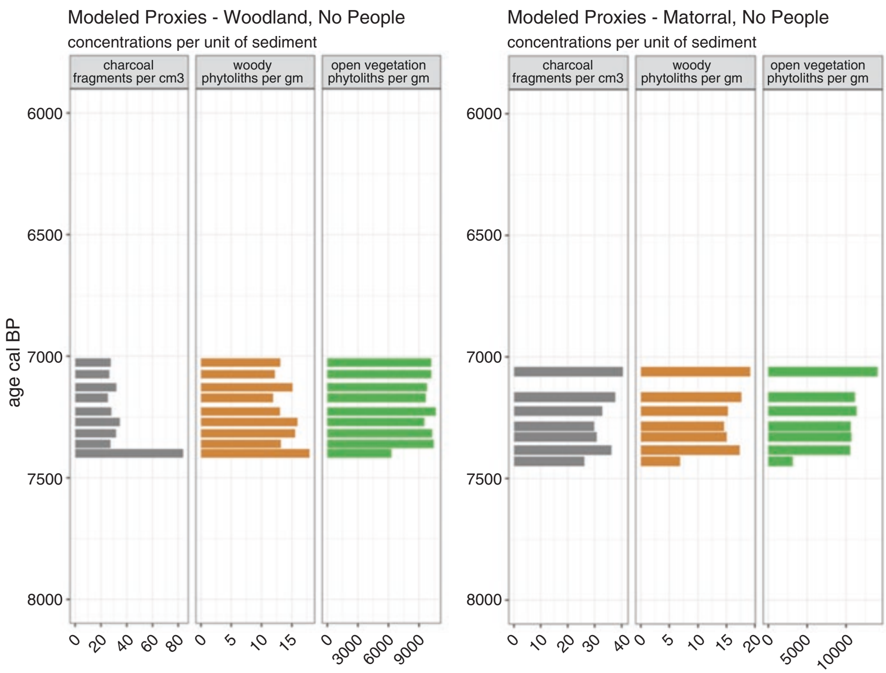

Fig. 10.6 Modeled digital proxies from MedLanD SES model output. Non-anthropogenic scenario experiments were initialized with Mediterranean woodland land cover and *matorral* shrubland land cover. Digital charcoal and phytolith concentrations are shown in units comparable to empirical proxies shown in Figs. 10.3 and 10.4

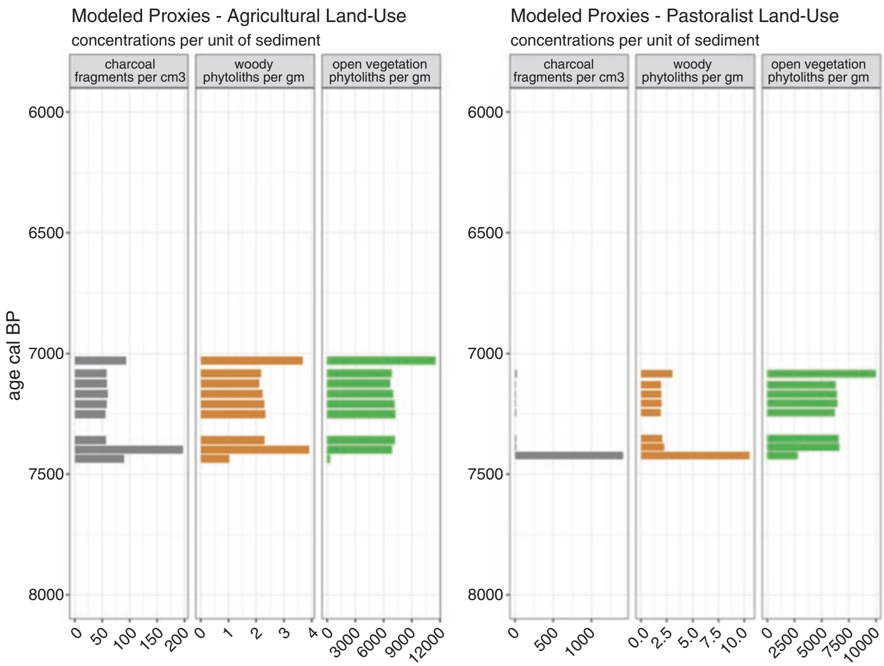

Fig. 10.7 Modeled digital proxies from MedLanD SES model output. Both anthropogenic land use scenario experiments (swidden agriculturalists and pastoralists – see Table 10.4 and text) were initialized with Mediterranean woodland land cover. Digital charcoal and phytolith concentrations are shown in units comparable to empirical proxies shown in Figs. 10.3 and 10.4

that, as with real-world deposits, some digital deposits are not as thick as others due to cumulative effects of erosion and deposition, and differential erosion and deposition rates resulted in a non-uniform distribution of the 10 cm digital samples through time.

This initial comparison is limited by the availability of empirical data as well as modeling procedures. As mentioned above, we have not yet completed analyses for cosmogenic nuclides, and the empirical sediment samples recovered were too small to contain sufficient micro-artifacts for analysis. Although it may be possible to calculate digital grain size categories from modeled overland flow, we have not yet done this. Hence, for the test reported here, we compare digital and empirical micro-charcoal and plant phytoliths from the modeled and real-world SP.NV.7 column location (Figs. 10.5, 10.6, and 10.7).

All model experiments produced quantities of digital proxies that agree closely with empirical concentrations of phytoliths and charcoal (Fig. 10.5), indicating that our proxy modeling protocol holds the potential to enable direct comparisons between complex, computational simulation models of SES and the empirical proxy data of the archaeological and paleoecological records. We set parameters in the MML to comparatively extreme values for land use practices to test whether

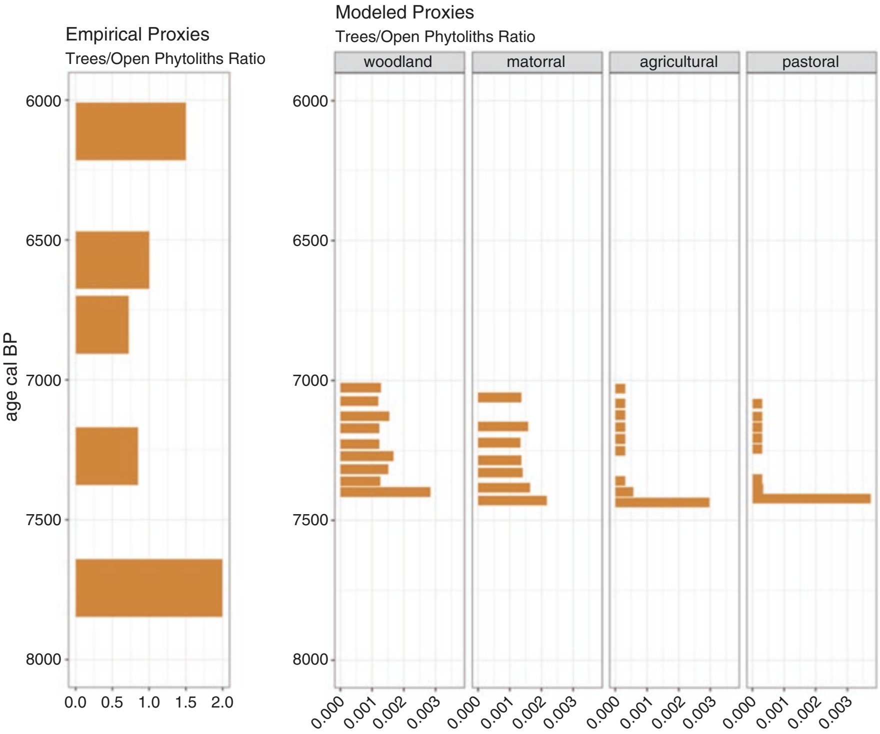

Fig. 10.8 Comparison of empirical phytoliths from core SP.NV.7 and four scenarios of modeled digital phytoliths: ratio of woody to open vegetation

different forms of land use and non-human landscape evolution would generate clearly different digital proxy records. Indeed, very different digital proxy records were generated from different non-human land cover and human land use scenarios (Figs. 10.5, 10.6, 10.7, 10.8, and 10.9). Both anthropogenic land use models (agricultural and pastoralist) were distinct from the non-human scenarios, creating degraded digital landscapes nearly devoid of trees. These differences can be seen clearly in the digital phytolith concentration values and woody/open vegetation index of Figs. 10.6, 10.7, and 10.8. Digital phytoliths from woody plants, especially, are over an order of magnitude less frequent in the agricultural and pastoral land use settings than in either the woodland or *matorral* scenarios due to land clearance for cultivation and ovicaprine grazing. Open vegetation phytolith concentrations are considerably more similar across all four modeling experiments. Digital charcoal accumulation tends to follow the concentrations of digital woody phytoliths. This mirrors the empirical charcoal record, heavily dominated by charcoal from woody plants (Fig. 10.2). Because there is less digital vegetation to burn in the degraded pastoralist scenario, the amount of digital charcoal is lower than in the other model experiments. Overall, these preliminary results show that digital phytoliths and charcoal are useful proxies for digital land cover under different land use scenarios,

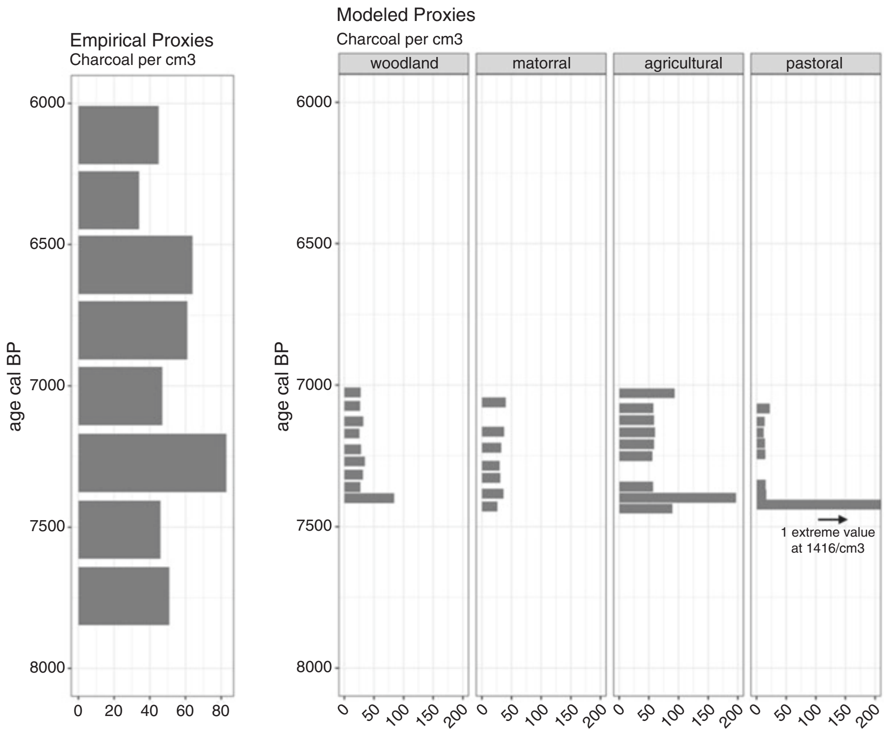

Fig. 10.9 Comparison of empirical phytoliths from core SP.NV.7 and four scenarios of modeled digital phytoliths: charcoal concentrations

meaning, in turn, that they provide a useful instrument for comparing and evaluating socio-ecological modeling results against an empirical record.

We did not expect any of the digital cores to closely match the corresponding empirical record dating to the early Neolithic from sediment column SP.NV.7 in this initial test of the protocol, and they do not (Figs. 10.8 and 10.9). Nonetheless, the differences between the empirical and digital proxies are informative, and there are also equally informative correspondences. The main differences between the empirical proxy record in sediment column SP.NV.7 and the digital proxy record from our SES modeling experiments in the same watershed basin fall into three categories.

First, we intentionally parameterized the human land use with comparatively extreme values to assess the potential of a digital core to differentiate different patterns of land use. As a result, the anthropogenic scenarios produce a rapid and significant decline in woody vegetation phytoliths, along with a spike in the amount of digital charcoal at the beginning of the modeling interval not seen in the empirical record – analogous to *landnám* clearance noted in the paleoecological record elsewhere in Europe (Edwards, 1993). Second, the ratios of woody to open vegetation phytoliths are several orders of magnitude lower in the digital proxy record than observed in the empirical samples (<0.001–0.002 for the digital phytoliths vs.

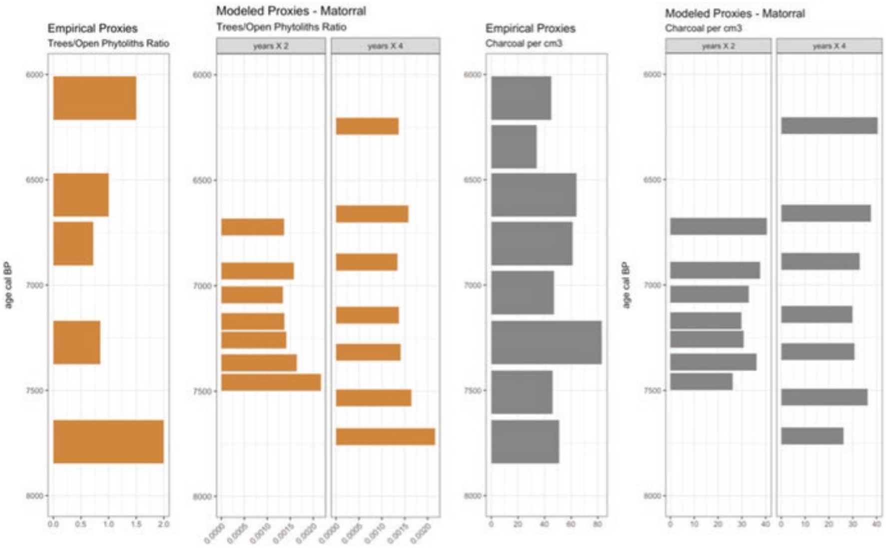

Fig. 10.10 Comparison of ratio of woody to open vegetation and charcoal from core SP.NV.7 and digital proxies from *matorral* scenario experiment (Table 10.4, Scenario 2) rescaled so that 1 modeled time step equals 2 calendar years and 4 calendar years

1.0–2.0 for the empirical phytoliths (Fig. 10.8). Finally, the temporal span of the digital core is much shorter and resolution much finer than the empirical sediment column. The digital core only overlaps one sediment sample with phytoliths and two with charcoal. We discuss all three of these differences below.

The two anthropogenic land use experiments that simulated degraded and denuded anthropogenic landscapes are the least similar to the empirical data. That is, neither of the anthropogenic model experiments likely represent past human land use in the mid-Holocene Canal de Navarrés valley. The two non-human experiments are more similar to the empirical data, suggesting that they better represent ancient land use. In fact, other archaeological and paleobotanical data indicate a very low-level human presence in this valley during the early Neolithic (Bernabeu Auban et al., 2014; Carrión & Van Geel, 1999; Snitker, 2018; Snitker et al., 2018). Nevertheless, the differences between the anthropogenic and non-anthropogenic digital records parallel that of empirical records elsewhere where rapid, fire-enabled human land clearance is thought to have taken place.

It is puzzling that the woody/open vegetation index is orders of magnitude lower for the simulation than for the empirical column (Fig. 10.8), given that total digital phytolith concentrations are in line with empirical concentrations (Fig. 10.5). This is the case even for the digital samples from the initialization phases of the modeling experiments, covered in Mediterranean woodland for the non-anthropogenic woodland scenario and both anthropogenic scenarios. We could attribute this to a need to retune the algorithms that generate digital phytoliths for woody and open vegetation, even though they are based on empirical data for phytolith accumulation rates.

An alternative explanation might be depositional and post-depositional processes affecting the empirical phytolith record that are not being simulated in our modeling experiments. Our proxy modeling algorithms simulate the generation and deposition of digital phytoliths from grassy and woody vegetation based solely on empirically observed phytolith generation rates. The only post-depositional process that affects the digital phytoliths is the erosion (i.e., removal) of some of the sediment layers in which they accumulate. However, a variety of biological and physical processes do affect the preservation of phytoliths after deposition (e.g., Cabanes and Shahack-Gross (2015), Esteban et al. (2017), Evett and Cuthrell (2013), Piperno (2006)). In this respect, the kind of proxy modeling described here, reflecting a more direct relationship between phytolith morphotypes proportions and vegetation cover, could potentially help calibrate phytolith proportions in real-world sediments where they may be altered by post-depositional processes.

Additionally, we note that both non-anthropogenic model experiments show a decline in woody vegetation after initialization. And though the woodland scenario begins with 100% coverage by a Mediterranean woodland and the *matorral* scenario begins with a shrub-dominated landscape, they both rapidly reach similar equilibria of woody/open vegetation ratios between 0.0010 and 0.0015. A close examination of modeling results suggests that the evolution of the modeled landscape to one dominated by sparse shrubs and open vegetation may be due to the frequency of natural (lightning-caused) fires that we simulated for the experiments reported here. We may have set this frequency higher than needed, creating numerous fires across the entire watershed that destroyed much (though not all) of the woody plants without any human intervention. Nevertheless, the empirical ratio of woody to open vegetation also drops by half after the oldest sample analyzed, paralleling the non-anthropogenic models.

Finally, we note the differences in temporal span and resolution between the modeled and empirical proxy records. Each model experiment ran for 500 time steps. While real-world landscape evolution processes (fires, rainfall, erosion/deposition, plant growth) take place continuously or at sub-annual intervals (e.g., rainfall), we have attempted to tune the modeling algorithms to simulate 1 year in a time step. Testing whether or not this parameterization does indeed simulate a calendar year requires empirical validation. For example, given a possible overabundance of lightning-cause fires that we noted, perhaps a model time step better represents several years of fire and plant regrowth. Figure 10.10 shows the effects of rescaling model output so that a model time step represents two or four real-world years, with the *matorral* scenario as an example. The rescaling where one model time step is equal to four calendar years, especially, shows a considerably better match with the empirical record for the simulation experiment initialized with *matorral* land cover and lacking human land use.

10.5 Conclusions

As quantitative and especially computational models come to play an increasingly important role in archaeological practice, we need to keep in mind that they are inherently no more or less accurate or useful than the inferential narrative models that have dominated the field since its inception. We also need to remember that *all* models are hypotheses about an empirically unknowable past. However, quantitative models are more explicit and transparent, making them more amenable to systematic evaluation than narrative inferential models. As deductive, first principle models, they also can help us build a better theory about human behavior and socio-ecological processes (Miller & Page, 2007). To realize these benefits, we will need to develop and systematically apply new ways to evaluate quantitative models using the empirical archaeological record.

While there has been some progress made in devising ways to compare quantitative model results against temporal snapshots of the spatial distribution of archaeological materials, one of the key contributions of archaeology to understanding human systems is its unique ability to study long-term change. It is important that we develop ways to test quantitative models of behavioral and socio-ecologic change against the archaeological record. We have reported on a new method for doing so, generating a time series of digital proxies that are directly comparable with archaeological and paleoecological proxies recovered from empirical stratigraphic contexts. Reporting on an initial proof-of-concept test of a protocol to generate such digital proxy data, we can show several important outcomes that are promising for this new method:

- Complex SES models can generate digital proxy data in concentrations equivalent to empirical proxies extracted from sediment samples.
- Models of long-term landscape dynamics representing different anthropogenic and non-anthropogenic scenarios can generate digital cores with distinct proxy records that correspond with landscape change in understandable ways.
- A digital proxy record can be usefully compared with a corresponding empirical record, in spite of issues with formation and post-depositional processes that can distort the empirical proxy record and issues with modeling algorithms that can distort model results. The fact that the non-anthropogenic digital proxy records best match the empirical one from the Canal de Navarrés valley is consistent with independent archaeological and paleoecological data from that region.
- Comparing digital and empirical proxy records can help guide the improvement of modeling algorithms and may also aid in correcting distortion in the empirical data.

Looking ahead, we plan to further refine the MML, adjusting the landscape fire algorithms, for example, and generate a suite of less extreme model parameterizations for anthropogenic land use to compare with the empirical record from the Canal de Navarrés valley and other study locales. We also will explore ways to aggregate repeated model runs (rather than using single exemplars like we did here) and represent variation across runs as a measure of uncertainty. We hope that the work reported here can inspire other archaeological modelers to think creatively about how to integrate this powerful new technology and the material record that has long been the basis of archaeological knowledge. We also hope this inspires empirical research designed to generate data that can be more useful for parameterizing and validating computational SES models, as well as supporting more traditional archaeological and paleoecological research.

10.6 Access to Data and Analysis

Data and analysis scripts used to generate the figures in this paper are openly accessible at https://zenodo.org/record/5567816 (Barton 2021)

Acknowledgments This research was supported by National Science Foundation: grants BCS-410269, DEB-1313727; DSI-NRF Centre of Excellence in Palaeosciences; Arizona State University School of Human Evolution and Social Change, Center for Social Dynamics & Complexity, School of Earth and Space Exploration; Universitat de València, Departament de Prehistòria, Arqueologia i Història Antiga; San Diego State University, Department of Anthropology; University of Witswaterand, Evolutionary Studies Institute; and the GRASS GIS Development Team.

References

Albert, R. M., & Weiner, S. (2001). Study of phytoliths in prehistoric ash layers from Kebara and Tabun caves using a quantitative approach. In J. D. Meunier & F. Colin (Eds.), *Phytoliths: Applications in earth sciences and human history* (pp. 251–266).

Altaweel, M. R., & Wu, Y. (2010). Route selection and pedestrian traffic: Applying an integrated modeling approach to understanding movement. *Structure and Dynamics, 4*.

Ammerman, A. J., & Cavalli-Sforza, L. L. (1971). Measuring the rate of spread of early farming in Europe. *Man, 6*, 674–688. https://doi.org/10.2307/2799190

Banning, E. B. (2010). Houses, households, and changing society in the Late Neolithic and Chalcolithic of the Southern Levant. *Paleorient, 36*, 46–87.

Barton, C. M. (2013). Stories of the past or science of the future? Archaeology and computational social science. In A. Bevan & M. W. Lake (Eds.), *Computational approaches to archaeological spaces* (pp. 151–178). University College London, Institute of Archaeology Publications. Left Coast Press.

Barton, C. M. (2016). From narratives to algorithms: Extending archaeological explanation beyond archaeology. In C. Isendahl & D. Stump (Eds.), *Oxford handbook of historical ecology and applied archaeology* (27pp). Oxford University Press.

Barton, CM. (2021). cmbarton/ProxyModeling_2021: RMarkdown script and data for Digital Proxies... paper 2021, *Zenodo*, 1.0, https://doi.org/10.5281/ZENODO.5567816.

Barton, C. M., Bernabeu Aubán, J., Aura Tortosa, J. E., & Garcia Puchol, O. (1999). Landscape dynamics and socioeconomic change: an example from the Polop Alto valley. *American Antiquity, 64*, 609–634.

Barton, C. M., Arrowsmith, R., Falconer, S., Fall, P., & Sarjoughian, H. S. (2004a). NSF-BCE-CNH: Landuse and landscape socioecology in the Mediterranean Basin: A natural laboratory for the study of the long-term interaction of human and natural systems. (BCS 410269).

Barton, C. M., Bernabeu Aubán, J., Aura Tortosa, J. E., & Molina Balaguer, L. (2004b). Historical contingency, nonlinearity, and the neolithization of the western Mediterranean. In L. Wandsnider & E. Athanassopoulos (Eds.), *Current issues in Mediterranean landscape archaeology* (pp. 99–124). University of Pennsylvania Press.

Barton, C. M., Bernabeu Auban, J., Garcia Puchol, O., Schmich, S., & Molina Balaguer, L. (2004c). Long-term socioecology and contingent landscapes. *Journal of Archaeological Method and Theory, 11*, 253–295. https://doi.org/10.1023/B:JARM.0000047315.57162.b7

Barton, C. M., Ullah, I. I. T., & Mitasova, H. (2010). Computational modeling and Neolithic socio-ecological dynamics: A case study from Southwest Asia. *American Antiquity, 75*, 364–386.

Barton, C. M., Ullah, I. I. T., Bergin, S. M., Mitasova, H., & Sarjoughian, H. (2012). Looking for the future in the past: Long-term change in socioecological systems. *Ecological Modelling, 241*, 42–53. https://doi.org/10.1016/j.ecolmodel.2012.02.010

Barton, C. M., Ullah, I. I., & Heimsath, A. (2015a). How to make a Barranco: Modeling erosion and land-use in Mediterranean landscapes. *Land, 4*, 578–606. https://doi.org/10.3390/land4030578

Barton, C. M., Ullah, I. I. T., Mayer, G. R., Bergin, S. M., Sarjoughian, H. S., & Mitasova, H. (2015b). MedLanD modeling laboratory v.1. Arizona State University, CoMSES Computational Model Library.

Barton, C. M., Ullah, I. I. T., Bergin, S. M., Sarjoughian, H. S., Mayer, G. R., Bernabeu-Auban, J. E., Heimsath, A. M., Acevedo, M. F., Riel-Salvatore, J. G., & Arrowsmith, J. R. (2016). Experimental socioecology: Integrative science for Anthropocene landscape dynamics. *Anthropocene, 13*, 34–45. https://doi.org/10.1016/j.ancene.2015.12.004

Bernabeu, J. (1993). El IIIr. Milenio a.C. en el País Valenciano. Los poblados de Jovades (Cocentaina. Alacant) y Arenal de la Costa (Ontinyent, Valencia). *Saguntum, 26*, 11–179.

Bernabeu Aubán, J., & Orozco Köhler, T. (2005). Mas d'Is (Penàguila, Alicante): Un recinto monumental del VI milenio cal AC. In P. Arias, R. Ontañón, & C. García-Moncó (Eds.), *III Congreso Sobre El Neolítico En La Península Ibérica (Santander, 2003)* (pp. 485–495). Instituto Internacional de Investigaciones Prehistóricas de Cantabria.

Bernabeu Aubán, J., Barton, C. M., Garcia, O., & La Roca, N. (1999). Prospecciones sistemáticas en el valle del Alcoi (Alicante): primeros resultados. *Arqueología Espacial, 21*, 29–64.

Bernabeu Auban, J., Orozco Köhler, T., Diez Castillo, A., & Gomez Puche, M. (2003). Mas d'Is (Penàguila, Alicante): aldeas y recintos monumentales del Neolítico Antiguo en el Valle del Serpis. *Trabajos de Prehistoria, 60*, 39–59.

Bernabeu Auban, J., Molina Balaguer, L., Díez Castillo, A., & Orozco Köhler, T. (2006). Inequalities and power. Three millennia of prehistory in Mediterranean Spain (5600–2000 cal BC). In P. Díaz del Río & L. L. García Sanjuan (Eds.), *Social inequality in Iberian late prehistory* (BAR international series) (pp. 97–116). Archaeopress.

Bernabeu Aubán, J., Molina Balaguer, L., Orozco Köhler, T., Diez Castillo, A., & Barton, C. M. (2006). Los Valles del Serpis (Alicante): 20 años de trabajos de campo. In M. S. Hernández Pérez, J. A. Soler Díaz, & J. A. López Padilla (Eds.), *Actas Del IV Congreso Del Neolítico Peninsular* (pp. 50–57). Museo Arqueológico de Alicante – MARQ.

Bernabeu Auban, J., Molina Balaguer, L., Orozco Köhler, T., Díaz Castillo, A., & Barton, C. M. (2008). Early neolithic at the Serpis Valley, Alicante, Spain. In M. Diniz (Ed.), *The early Neolithic in the Iberian Peninsula. Regional and transregional components. Proceedings of the XV World Congress (Lisbon, 2006)* (International Series) (pp. 53–59). BAR.

Bernabeu Auban, J., Barton, C. M., García Puchol, O., Diez Castillo, A., & Pardo Gordó, S. (2014). Prospecciones en la Canal de Navarrés: Campaña 2014. Servei de Patrimoni. Consellería de Cultura, Generalitat Valenciana, Valencia.

Bernabeu, J., Pascual, J. L., Orozco, T., Badal, E., Fumanal, M. P., & García Puchol, O. (1994). Niuet (L'Alquería d'Asnar). Poblado del IIIr milenio a.C. *Recerques del Museu d'Alcoi, 3*, 9–74.

Bevan, A., & Conolly, J. (2004). GIS, archaeological survey, and landscape archaeology on the Island of Kythera, Greece. *Journal of Field Archaeology, 29*, 123–138. https://doi.org/10.1179/jfa.2004.29.1-2.123

Bonet, A. (2004). Secondary succession of semi-arid Mediterranean old-fields in South-Eastern Spain: Insights for conservation and restoration of degraded lands. *Journal of Arid Environments, 56*, 213–233.

Bonet, A., & Pausas, J. G. (2007). Old field dynamics on the dry side of the Mediterranean Basin: Patterns and processes in semiarid SE Spain. In V. A. Cramer & R. J. Hobbs (Eds.), *Old fields: Dynamics and restoration of abandoned farmland* (pp. 247–264). Island Press.

Box, G. E. (1979). Robustness in the strategy of scientific model building. In R. Launer & G. Wilkinson (Eds.), *Robustness in statistics* (pp. 201–236). Academic.

Cabanes, D., & Shahack-Gross, R. (2015). Understanding fossil Phytolith preservation: The role of partial dissolution in paleoecology and archaeology. *PLoS One, 10*, e0125532. https://doi.org/10.1371/journal.pone.0125532

Carrión, J. S., & Van Geel, B. (1999). Fine-resolution Upper Weichselian and Holocene palynological record from Navarrés (Valencia, Spain) and a discussion about factors of Mediterranean forest succession. *Review of Palaeobotany and Palynology, 106*, 209–236. https://doi.org/10.1016/S0034-6667(99)00009-3

Carter, J., Howden, S., Day, K., McKeon, G., (1998). *Soil carbon, nitrogen and phosphorous and biodiversity in relation to climate change, evaluation of the impact of climate change on northern Australian grazing industries*, vol. 139A. Final report for the Rural Industries Research and Development Corporation on Project DAQ.

Chamberlin, T. C. (1890). The method of multiple working hypotheses. *Science, 15*, 92–96.

Clark, J. S. (1988). Particle motion and the theory of charcoal analysis: Source area, transport, deposition, and sampling. *Quaternary Research, 30*, 67–80. https://doi.org/10.1016/0033-5894(88)90088-9

Codding, B. F., & Bird, D. W. (2015). Behavioral ecology and the future of archaeological science. *Journal of Archaeological Science*. https://doi.org/10.1016/j.jas.2015.02.027

Diez Castillo, A., Barton, C. M., La Roca Cervigón, N., & Bernabeu Auban, J. (2008). Landscape Socioecology in the Serpis Valley (10,000–4000 BP). in *Layers of perception. Proceedings of the 35th international conference on computer applications and quantitative methods in archaeology (CAA)* (Berlin, Germany, April 2–6, 2007). Presented at the conference on computer applications and quantitative methods in archaeology (CAA), Dr. Rudolf Habelt GmbH, Berlin, pp. 1–7.

Diez Castillo, A., Bernabeu Aubán, J., Barton, C. M., García Puchol, O., Bergin, S.M., & Pardo Gordó, S., 2014. *Paperless survey? New methodological approaches to archaeological fieldwork, the case of La Canal de Navarrés*. Presented at the making sense of archaeological survey, Instituto Universitario de Investigación en Arqueología Ibérica Universidad de Jaén.

Edwards, K. J. (1993). Models of mid-Holocene forest farming for North-West Europe. In F. M. Chambers (Ed.), *Climate change and human impact on the landscape* (pp. 132–145). Chapman and Hall.

Esteban, I., De Vynck, J. C., Singels, E., Vlok, J., Marean, C. W., Cowling, R. M., Fisher, E. C., Cabanes, D., & Albert, R. M. (2017). Modern soil phytolith assemblages used as proxies for Paleoscape reconstruction on the south coast of South Africa. *Quaternary International, 434*, 160–179. https://doi.org/10.1016/j.quaint.2016.01.037

Evett, R. R., & Cuthrell, R. Q. (2013). Phytolith evidence for a grass-dominated prairie landscape at Quiroste Valley on the Central Coast of California. *California Archaeology, 5*, 319–335. https://doi.org/10.1179/1947461X13Z.00000000017

Flannery, K. V. (1993). Will the real model please stand up: comments on Saidel's 'Round house or square'. *Journal of Mediterranean Archaeology, 6*, 109–117.

Flinn, D., Hopmans, P., Farrell, P., & James, J. (1979). Nutrient loss from the burning of Pinus radiata logging residue. *Australian Forest Research, 9*, 17–23.

Forbes, M. S., Raison, R. J., & Skjemstad, J. O. (2006). Formation, transformation and transport of black carbon (charcoal) in terrestrial and aquatic ecosystems. *Science of the Total Environment, 370*, 190–206. https://doi.org/10.1016/j.scitotenv.2006.06.007

Fort, J., Pujol, T., & Linden, M. (2012). Modelling the Neolithic transition in the Near East and Europe. *American Antiquity, 77*, 203–219. https://doi.org/10.7183/0002-7316.77.2.203

Fredlund, G. G., & Tieszen, L. T. (1994). Modern Phytolith assemblages from the North American Great Plains. *Journal of Biogeography, 21*, 321–335. https://doi.org/10.2307/2845533

Freeman, J., Hard, R. J., & Mauldin, R. P. (2017). A theory of regime change on the Texas Coastal Plain. *Quaternary International*. https://doi.org/10.1016/j.quaint.2016.12.029

García Puchol, O., & Aura Tortosa, J. E. (Eds.). (2006). El Abric de la Falguera (Alcoi, Alacant). 8.000 años de ocupación humana en la cabecera del rio Alcoi. CAM (Caja de Ahorros del Mediterráneo) y Ajuntament d'Alcoi, Alicante.

García Puchol, O., Barton, C. M., & Bernabeu Aubán, J. (2008). Programa de prospección geofísica, microsondeos y catas para la caracterización de un gran foso del IV milenio cal AC en Alt del Punxó (Muro de L'Alcoi, Alacant). *Trabajos de Prehistoria, 65*, 143–154. https://doi.org/10.3989/tp.2008.v65.i1.140

García Puchol, O., Barton, M., Bernabeu Aubán, J., Diez Castillo, A., & Pardo Gordò, S. (2014). De la prospección sistemática al laboratorio GIS en La Canal de Navarrés. *SAGVNTVM. Papeles del Laboratorio de Arqueología de Valencia, 46*, 209–214. https://doi.org/10.7203/SAGVNTVM.46.4239

Gholami, S., Sarjoughian, H. S., Godding, G. W., Peters, D. R., & Chang, V. (2014). Developing composed simulation and optimization models using actual supply-demand network datasets. In: *Simulation conference (WSC), 2014 Winter*. Presented at the simulation conference (WSC), 2014 Winter, pp. 2510–2521. https://doi.org/10.1109/WSC.2014.7020095.

Gremillion, K. J. (2002). Foraging theory and hypothesis testing in archaeology: An exploration of methodological problems and solutions. *Journal of Anthropological Archaeology, 21*, 142–164. https://doi.org/10.1006/jaar.2001.0391

Grimm, V., Revilla, E., Berger, U., Jeltsch, F., Mooij, W. M., Railsback, S. F., Thulke, H.-H., Weiner, J., Wiegand, T., & DeAngelis, D. L. (2005). Pattern-oriented modeling of agent-based complex systems: Lessons from ecology. *Science, 310*, 987–991. https://doi.org/10.1126/science.1116681

IVIA. (2015). *Weather Station wind data from the canal de Navarrés*. Instituto Valenciano de Investigaciones Agrarias.

Katz, O., Cabanes, D., Weiner, S., Maeir, A. M., Boaretto, E., & Shahack-Gross, R. (2010). Rapid phytolith extraction for analysis of phytolith concentrations and assemblages during an excavation: An application at Tell es-Safi/Gath, Israel. *Journal of Archaeological Science, 37*, 1557–1563. https://doi.org/10.1016/j.jas.2010.01.016

Keene, A. S. (1983). 6 – Biology, behavior, and borrowing: A critical examination of optimal foraging theory in archaeology. In J. A. Moore & A. S. Keene (Eds.), *Archaeological hammers and theories* (pp. 137–155). Academic. https://doi.org/10.1016/B978-0-12-505980-0.50014-8

Kohler, T. A., & van der Leeuw, S. E. (2007). *The model-based archaeology of socionatural systems*. School for Advanced Research Press.

Kohler, T. A., Bocinsky, R. K., Cockburn, D., Crabtree, S. A., Varien, M. D., Kolm, K. E., Smith, S., Ortman, S. G., & Kobti, Z. (2012). Modelling prehispanic Pueblo societies in their ecosystems. *Ecological Modelling, 241*, 30–41. https://doi.org/10.1016/j.ecolmodel.2012.01.002

Le, J., & Shackleton, N. J. (1994). Reconstructing paleoenvironment by transfer function: Model evaluation with simulated data. *Marine Micropaleontology, 24*, 187–199. https://doi.org/10.1016/0377-8398(94)90021-3

Lemmen, C., Gronenborn, D., & Wirtz, K. W. (2011). A simulation of the Neolithic transition in Western Eurasia. *Journal of Archaeological Science, 38*, 3459–3470. https://doi.org/10.1016/j.jas.2011.08.008

Mayer, G. R., & Sarjoughian, H. S. (2009). Composable cellular automata. *Simulation, 85*, 735–749. https://doi.org/10.1177/0037549709106341

Miller, J. H., & Page, S. E. (2007). *Complex adaptive systems: An introduction to computational models of social life*. Princeton University Press.

Mitasova, H., Barton, C. M., Ullah, I. I. T., Hofierka, J., & Harmon, R. S. (2013). GIS-based soil erosion modeling. In J. Shroder & M. Bishop (Eds.), *Treatise in geomorphology* (Remote sensing and GI science in geomorphology) (Vol. 3, pp. 228–258). Academic.

Neumann, K., Strömberg, C. A. E., Ball, T., Albert, R. M., Vrydaghs, L., & Cummings, L. S. (2019). International code for Phytolith nomenclature (ICPN) 2.0. *Annals of Botany, 124*, 189–199. https://doi.org/10.1093/aob/mcz064

Parnell, A. C., Haslett, J., Allen, J. R. M., Buck, C. E., & Huntley, B. (2008). A flexible approach to assessing synchroneity of past events using Bayesian reconstructions of sedimentation history. *Quaternary Science Reviews, 27*, 1872–1885. https://doi.org/10.1016/j.quascirev.2008.07.009

Parnell, A. C., Buck, C. E., & Doan, T. K. (2011). A review of statistical chronology models for high-resolution, proxy-based Holocene palaeoenvironmental reconstruction. *Quaternary Science Reviews, 30*, 2948–2960. https://doi.org/10.1016/j.quascirev.2011.07.024

Perry, G. L. W., & O'Sullivan, D. (2018). Identifying narrative descriptions in agent-based models representing past human-environment interactions. *Journal of Archaeological Method and Theory, 25*, 795–817. https://doi.org/10.1007/s10816-017-9355-x

Piperno, D. R. (2006). *Phytoliths: A comprehensive guide for archaeologists and paleoecologists*. Rowman Altamira.

Riris, P. (2018). Assessing the impact and legacy of swidden farming in neotropical interfluvial environments through exploratory modelling of post-contact Piaroa land use (Upper Orinoco, Venezuela). *The Holocene, 28*, 945–954. https://doi.org/10.1177/0959683617752857

Robinson, D. T., Di Vittorio, A., Alexander, P., Arneth, A., Barton, C. M., Brown, D. G., Kettner, A., Lemmen, C., O'Neill, B. C., Janssen, M., Pugh, T. A. M., Rabin, S. S., Rounsevell, M., Syvitski, J. P., Ullah, I., & Verburg, P. H. (2018). Modelling feedbacks between human and natural processes in the land system. *Earth System Dynamics, 9*, 895–914. https://doi.org/10.5194/esd-9-895-2018

Rogers, J. D., & Cegielski, W. H. (2017). Opinion: Building a better past with the help of agent-based modeling. *Proceedings of the National Academy of Sciences, 114*, 12841–12844. https://doi.org/10.1073/pnas.1718277114

Romanowska, I., Wren, C. D., & Crabtree, S. A. (2021). *Agent-based modeling for archaeology: Simulating the complexity of societies*. SFI Press.

Sarjoughian, H., Smith, J., Godding, G., & Muqsith, M. (2013). Model composability and execution across simulation, optimization, and forecast models. In *Proceedings of the symposium on theory of modeling & simulation-DEVS integrative M&S symposium* (p. 30). Society for Computer Simulation International.

Sarjoughian, H. S., Meyer, G. R., Ullah, I. I., & Barton, C. M. (2015). Managing hybrid model composition complexity: Human–environment simulation models. In L. Yilmaz (Ed.), *Concepts and methodologies for modeling and simulation, simulation foundations, methods and applications* (pp. 107–134). Springer International Publishing.

Schiffer, M. B. (1987). *Formation processes of the archaeological record*. University of New Mexico Press.

Smith, E. A., Bettinger, R. L., Bishop, C. A., Blundell, V., Cashdan, E., Casimir, M. J., Christenson, A. L., Cox, B., Dyson-Hudson, R., Hayden, B., Richerson, P. J., Roth, E. A., Simms, S. R., & Stini, W. A. (1983). Anthropological applications of optimal foraging theory: A critical review [and comments and reply]. *Current Anthropology, 24*, 625–651.

Snitker, G. (2018). Identifying natural and anthropogenic drivers of prehistoric fire regimes through simulated charcoal records. *Journal of Archaeological Science, 95*, 1–15. https://doi.org/10.1016/j.jas.2018.04.009

Snitker, G. (2019). *Anthropogenic fire and the development of Neolithic agricultural landscapes: Connecting archaeology, paleoecology, and fire science to evaluate human impacts on fire regimes (PhD dissertation)*. Arizona State University.

Snitker, G. (2020). The Charcoal Quantification Tool (CharTool): A Suite of Open-source Tools for Quantifying Charcoal Fragments and Sediment Properties in Archaeological and Paleoecological Analysis. Ethnobiology Letters, 11, 103–115. https://doi.org/10.14237/ebl.11.1.2020.1653.

Snitker, G., Castillo, A. D., Barton, C. M., Aubán, J. B., Puchol, O. G., & Pardo-Gordó, S. (2018). Patch-based survey methods for studying prehistoric human land-use in agriculturally modified landscapes: A case study from the Canal de Navarrés, Eastern Spain. *Quaternary International, Geoarchaeology: A toolbox for revealing latent data in sedimentological and archaeological records, 483*, 5–22. https://doi.org/10.1016/j.quaint.2018.01.034

Tsartsidou, G., Lev-Yadun, S., Albert, R.-M., Miller-Rosen, A., Efstratiou, N., & Weiner, S. (2007). The phytolith archaeological record: Strengths and weaknesses evaluated based on a quantitative modern reference collection from Greece. *Journal of Archaeological Science, 34*, 1262–1275. https://doi.org/10.1016/j.jas.2006.10.017

Ullah, I. I. T. (2017). *The consequences of human land-use strategies during the PPNB-LN transition: A simulation modeling approach, anthropological research papers, 60*. Arizona State University.

Ullah, I. I. T., & Bergin, S. (2012). Modeling the consequences of village site location: Least cost path modeling in a coupled GIS and agent-based model of village agropastoralism in Eastern Spain. In D. A. White & S. L. Surface-Evans (Eds.), *Least cost analysis of social landscapes: Archaeological case studies* (pp. 155–173). University of Utah Press.

van der Leeuw, S. E. (2004). Why model? *Cybernetics and Systems: An International Journal, 35*, 117–128. https://doi.org/10.1080/01969720490426803

Verburg, P. H., Dearing, J. A., Dyke, J. G., van der Leeuw, S., Seitzinger, S., Steffen, W., & Syvitski, J. (2016). Methods and approaches to modelling the Anthropocene. *Global Environmental Change, 39*, 328–340. https://doi.org/10.1016/j.gloenvcha.2015.08.007

Watts, J., & Ossa, A. (2016). Exchange network topologies and agent-based modeling: Economies of the sedentary-period Hohokam. *American Antiquity, 81*, 623–644. https://doi.org/10.1017/S0002731600101003

Wells, H. G., & Roger. (1895). *The time machine, Oxford World's classics*. William Heinemann.

Wurzer, Gabriel., Kowarik, Kerstin., & Reschreiter, Hans. (Eds.). (2015). *Agent-based Modeling and Simulation in Archaeology.* Springer.

Zurro, D. (2018). One, two, three phytoliths: Assessing the minimum phytolith sum for archaeological studies. *Archaeological and Anthropological Sciences, 10*, 1673–1691. https://doi.org/10.1007/s12520-017-0479-4